Hindawi
Journal of Electrical and Computer Engineering
Volume 2023, Article ID 9611321, 25 pages
https://doi.org/10.1155/2023/9611321

Research Article

Internet of Things Enabled Intelligent Automation for Smart Home with the Integration of PSO Algorithm and PID Controller

Rajesh Singh,[1,2] **Anita Gehlot**,[1,2] **Piyush Kuchhal**,[3] **Sushabhan Choudhury**,[3] **Shaik Vaseem Akram**,[1,4] **Neeraj Priyadarshi**,[5] **and Baseem Khan**[2,6]

[1]*Department of Research and Innovation, Uttaranchal Institute of Technology, Uttaranchal University, Dehradun 248007, India*
[2]*Department of Project Management, Universidad Internacional Iberoamericana, Campeche, CP 24560, Mexico*
[3]*University of Petroleum and Energy Studies, Dehradun, Uttarakhand, India*
[4]*Law College Dehradun, Uttaranchal University, Dehradun 248007, India*
[5]*Department of Electrical Engineering, JIS College of Engineering, Kolkata 741235, India*
[6]*Department of Electrical and Computer Engineering, Hawassa University, Hawassa, Ethiopia*

Correspondence should be addressed to Baseem Khan; baseem.khan04@ieee.org

Received 12 May 2022; Revised 15 February 2023; Accepted 25 February 2023; Published 28 March 2023

Academic Editor: Mohamed Louzazni

Currently, due to the widespread population growth, there is a widespread concern about an electricity shortage. As a result, smart devices have evolved and gained significant attention to reduce power consumption in home appliances due to electricity shortages. However, it lacks a universal remote control that can control home appliances based on environmental conditions. To overcome these challenges, this study proposed a hardware-based remote-control system that operates both in autonomous and semiautonomous modes to control home appliances based on environmental conditions. In the autonomous mode, the receiver section regulates the parameters under ambient conditions by varying the appliance's applied voltage levels via a dimmer. The parameters in semiautonomous are monitored by the user via various levels of remote control. A 2.4 GHz RF modem is used to establish wireless personal network (WPAN) communication between the remote and the receiver. In addition, a Wi-Fi modem is built into the receiver to enable internet-based mobile applications to operate appliances. During the MATLAB analysis, a proportional integral derivative (PID) controller with a particle swarm optimization (PSO) method was found as a superior approach to control the home appliance with adequate environmental conditions. It is concluded from the MATLAB study that the PSO-PID controller delivered an energy saving of 14.88% for the heater, 36.9% for the exhaust fan, and 37.49% for the light bulb compared to the conventional appliances.

1. Introduction

At present, India is one of the top three countries in terms of energy generation, with 1,547 Terawatt-hour (TWh) and 1,309 TWh consumption, respectively [1, 2]. Over the last decade, electricity consumption has increased by 73% due to the rapid population growth and it led to the power shortage faced by India, i.e., 70,000 Mega Watt (MW) [3]. The challenge of power shortages can be handled in two ways as follows: the first is to employ more traditional renewable energy sources to generate more electricity [4] and the second is to optimize the use of available electricity by smart appliances [5]. Technological advancements have empowered the development of smart devices not only to minimize power usage but also energy waste. Integrating smart devices into the home environment [6] led to the evolution of smart home automation in which devices are automatically controlled. Yet, there is a lack of common protocol to control multiple devices through a single controller with reliability and flexibility in home automation [2]. A home is similar to a system with several physical parameters that depend on each other and the environment. It is observed as a subsystem that exhibits linear or nonlinear dynamic behaviors [7]. The complexity of the control operation increases as

there are changes in the internal behavior and environment in the building. Due to growing environmental concerns, control systems play an important role in reducing energy consumption without compromising comfort goals [8].

A control system is a set of commands to regulate the behavior of a device, and a control system can be open-loop or closed-loop [9]. In previous studies, the control system is interconnected with the components of the home to control the appliances. However, this approach resulted in unreliable, inaccurate performance and is difficult to sense the changes in the external environment [10]. To overcome these limitations, open-loop and closed-loop controls are used. Open-loop control shows the actual operation of the system according to the input signal, but a closed-loop system is used for the desired output with different input signals [11]. A PID controller is utilized as a control system to control appliances by tuning the parameters [12, 13].

Reference [14] concludes that optimization is a critical notion in engineering for realizing the end product to reduce power consumption, boost yield, cost, and time delay. Moreover, optimization is carried out in the field of engineering because of challenges due to discontinuity, nonlinearity, and nondifferentiability. In reference [15], to obtain sufficient matching factors for the system's derivation, many computational operations are essential for hardware devices. Many optimization techniques are implemented to minimize computational complexity. For hardware-compatible optimization methodologies, genetic algorithm (GA) and PSO algorithms have been considered for determining the right tuning parameters. The authors in [16] conducted a study in which they integrated PSO and GA-PSO to create two resource allocation techniques to increase system performance by enabling up to two device-device pairs to share the same frequency with one cellular user equipment. In reference [17], the analytical framework is used to capture a wide range of properties of optimization algorithm implementations in PSO hardware (Field Programmable Gate Arrays) and software, with a focus on outperforming similar state-of-the-art implementations. It is also concluded that optimization algorithms can be adopted in the hardware devices for overcoming the issues faced due to discontinuity, nonlinearity, and nondifferentiability. As a part of controlling home appliances, a PID controller is implemented for tuning the parameters in order of implementing the autonomous and semiautonomous mode-based system.

With the motivation of the previous facts, this study aims to implement an intelligent remote-control system with hardware to control home appliances in autonomous and semiautonomous modes, based on environmental conditions variation. A MATLAB analysis is carried out to conclude which PID controller based on different algorithms can be implemented in the hardware for autonomous and semiautonomous modes. The study implemented the GA and PSO algorithms to check the optimal optimization algorithm for implementing the PID controller effectively for autonomous and semiautonomous modes for controlling home appliances. The novelty of the proposed system is implementing the customized hardware system for controlling the appliances with a PID controller and tuning parameters for implementing a semiautonomous mode. The contribution of the study is as follows:

(i) Customized hardware with 2.4 GHz RF and Wi-Fi communication capability is implemented for wireless connectivity establishment between remote and receiver sections for autonomous and semi-autonomous operation.

(ii) A MATLAB analysis is carried out and identified which particular optimization algorithms are optimal in tuning parameters of hardware.

(iii) The experimental results conclude that the PSO-PID controller delivered an energy saving of 14.88% for the heater, 36.9% for the exhaust fan, and 37.49% for the light bulb compared to conventional appliances.

(iv) The current consumption analysis of remote and receiver hardware is also analyzed in this study.

The structure of the study is as follows: Section 2 is a review of the literature; Section 3 is a detailed description of the working of the system using block diagrams. Section 4 covers the PID controller and optimization algorithm. Section 5 covers the programming flow diagram of semi-autonomous mode, autonomous mode, and receiver. Section 6 covers the calibration of sensors with instruments. Section 7 covers the experimental outcomes of a heater, bulb, and exhaust fan along with power consumption analysis. Section 8 covers a conclusion and the future scope of the system.

2. Literature Review

In this section, we discuss the distinct techniques that have been implemented in the home to control the appliances and minimize energy consumption. A wireless sensor network-based thermal comfort system is implemented to maintain room temperature as the environment changes, and results are obtained with neuro-fuzzy and PSO [18]. An intelligent monitoring system has been implemented to monitor various parameters of the home environment by integrating Zigbee and Global System for Mobile Communication (GSM) technology [19]. The PID controller was modified to use PSO with an automatic voltage change that has increased the system's efficiency [20]. A method is proposed to achieve an efficient output voltage or high switching frequency based on an inverter and the PID methods with the lowest ripple content [21, 22]. A comparative study of ant colony optimizations (ACOs) using the genetic algorithm and the Ziegler–Nichols method was discussed and concluded that ACOs are a better option [23]. To efficiently manage energy consumption, an android smartphone-based remote control for the home energy management system is proposed to dim the liquid emitting diode (LED) [21, 24]. A genetic algorithm for automatic control of PID controller in heating, ventilation, and air conditioning (HVAC) systems is carried out, and it is concluded that the genetic algorithm delivered the best performance [25]. A method was suggested by a study to

determine which of the three optimization methods is best for tuning PIDC controllers for automatic voltage regulators [26].

A ZigBee-based smart energy management system is proposed with the help of a motion sensor and power consumption settling time to reduce power consumption [27, 28]. IoT-based and ZigBee-based wireless sensor network (WSN) is implemented to monitor environmental parameters such as temperature, humidity, meter readings, and light [29, 30]. An integrated WSN with bee moths and Meshlium gateway was implemented to conserve energy by regulating light strength with pulse width modulation (PWM) [31]. IoT talk remote control (IoTtalkRC) is a mechanism that uses sensors to replace infrared remote controls as universal software-defined remote controls for aftermarket appliances [32, 33]. A prototype has been developed to perform remote control and performance evaluation of ECHONET-compatible smart home devices [34, 35]. GSM and Bluetooth-enabled remote monitoring system is developed through an android-based graphical user interface (GUI) [36, 37]. Open NFC touch and control (NTCP) is a tool that allows users to replace home appliances and devices of home appliances with smartphones to use universal remote controls [38]. Intelligent remote control, which controls and operates all home devices via the Internet via a mobile app, has independent learning capabilities and acts as a microcontroller for the ESP8266 [39]. With the integration of Wi-Fi and radio frequency, a voice- and wireless-based smart home management system is presented. To make the system more approachable, two sets of control schemes—voice control and button control—are created by the functional requirements of the system [40]. An IoT-inspired intelligent smart home control system is implemented to monitor and control the security of the home through a mobile application [41, 42]. In reference [43], authors presented the design and implementation of the energy efficient home automation system. Table 1 presents the comparative analysis of the current study, with the other studies that implemented the home automation-based system with IoT. It has been observed that the most recent studies have implemented the Wi-Fi-based module such as ESP 8266, which has limitations in power consumption. The significant parameter that is included in the comparative table is a mode of automation, where semiautonomous-based automation is implemented in a wide range. However, a current study implemented a network of 2.4 GHz RF and Wi-Fi for the implementation of autonomous and semiautonomous systems in controlling home appliances. Moreover, this study has calibrated the sensor and also optimized the proposed hardware as it is limitedly implemented in the previous studies.

From the literature review, it is concluded that the PID controller can be utilized to control the home appliance system. The power consumption is minimized by using optimization techniques with a PID controller. Moreover, it is concluded from the review that the ZigBee network can be used to implement the autonomous mode. It is also concluded that optimization algorithms can be adopted in the hardware devices for overcoming the issues faced due to discontinuity, nonlinearity, and nondifferentiability.

3. System Development

An IoT-assisted architecture is proposed to implement remote control in autonomous and semiautonomous modes (Figure 1). The system is divided into two parts, a receiver section and the remote control. The remote control is used to control the receiver section, connected to the appliances to be controlled. In autonomous mode, the receiver section controls the parameters under ambient circumstances by varying the applied voltage levels of the appliance through a dimmer.

In semiautonomous, the parameters are monitored by the user via various levels of remote control. A 2.4 GHz RF modem is used to establish wireless personal network (WPAN) communication between the remote and the receiver. A Wi-Fi modem is integrated with the receiver to activate the control of appliances through the mobile application based on the Internet. The significance and function of the receiver section and remote section are discussed in the following section with a block diagram.

3.1. Remote Control. The remote control shown in Figure 2 comprises of temperature/humidity (T/H) sensor, light-dependent resistors (LDRs), ATmega16, RF modem, LCD $16 * 2$ display unit, switches, and battery. The switch array is used to control the appliances. The temperature/humidity sensor provides temperature and humidity information as a feedback signal to the system. The remote control has nine switches for various operations.

Two switches are for mode selection of operation as semiautonomous or autonomous mode. Three pairs of up/down keys are kept in the remote control to increase/decrease the three parameters, namely, exhaust fan speed, heater temperature, and light intensity. The "OK" switch is used to deliver the information packet to the receiver section, and switch multiplexing is utilized to reduce the number of switches by using the same keys for level shifting on all appliances. A li-ion battery is used as a power supply module for remote control, and all the devices at the remote-control end operate at a +5 V DC power supply.

3.2. Receiver Section. Figure 3 shows the receiver board comprised of a three-dimmer circuit, ATmega 16 microcontroller, RF modem, LCD $16 * 2$ display unit, power supply, exhaust fan (EF), heater (H), and bulb (B). Dimming circuits are useful to control the dimming levels of the exhaust fan, heater, and bulb.

PID controller is implemented with a dimmer in the receiver section to control the dimming of room appliances, by setting the firing angle. The receiver section will receive a packet that contains the data from the remote control in the form of temperature, humidity, and light intensity. If the packet contains the data of temperature, then the corresponding error signal is generated and then provides the signal to the PID controller to control the temperature of the heater. The same is the case with the humidity and light intensity. In addition, the receiver section is connected to the mobile app through the Internet and cloud server. The

Table 1: Comparison of the current study with previous studies.

References	Objectives	Hardware	Communication	Mode of automation
[41]	Controlling the electrical appliances with environmental monitoring	ESP 8266 Wi-Fi and gateway-based hardware	Wi-Fi	Semiautonomous
[44]	Controlling home appliances with sensors and smartphone	Raspberry PI and Arduino mega	Wi-Fi	Semiautonomous
[45]	Intelligent decision-making for identifying the status of devices	Raspberry Pi	GSM	Autonomous
[46]	Automated the control of home appliances over the Internet anytime and anywhere	NODE MCU	Wi-Fi	Semiautonomous
Proposed study	Implemented optimization algorithm for the hardware in implementing home automation system	Customized hardware based on ATmega 16	2.4 GHz RF and Wi-Fi	Autonomous and semiautonomous

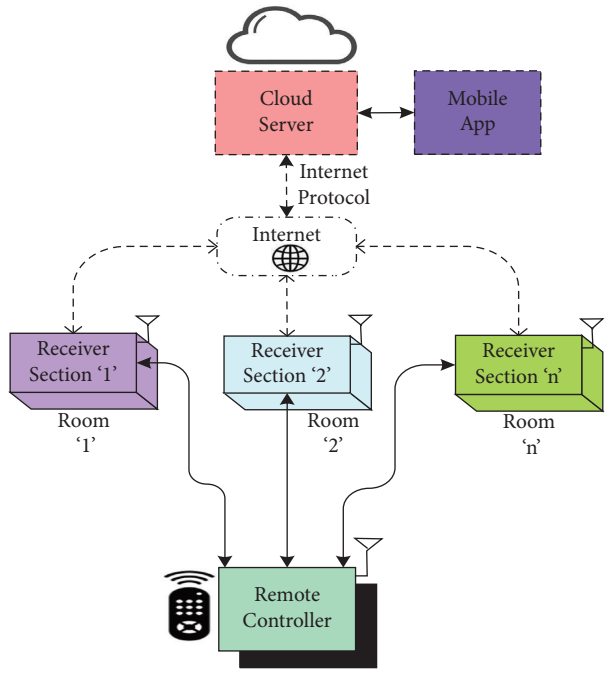

Figure 1: IoT-enabled architecture for remote controller.

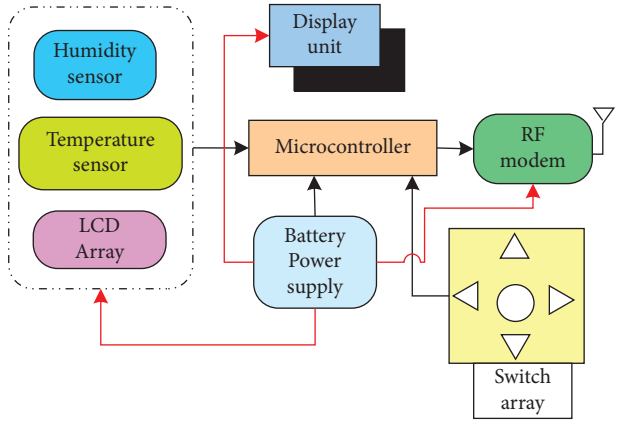

Figure 2: Block diagram of a remote controller section.

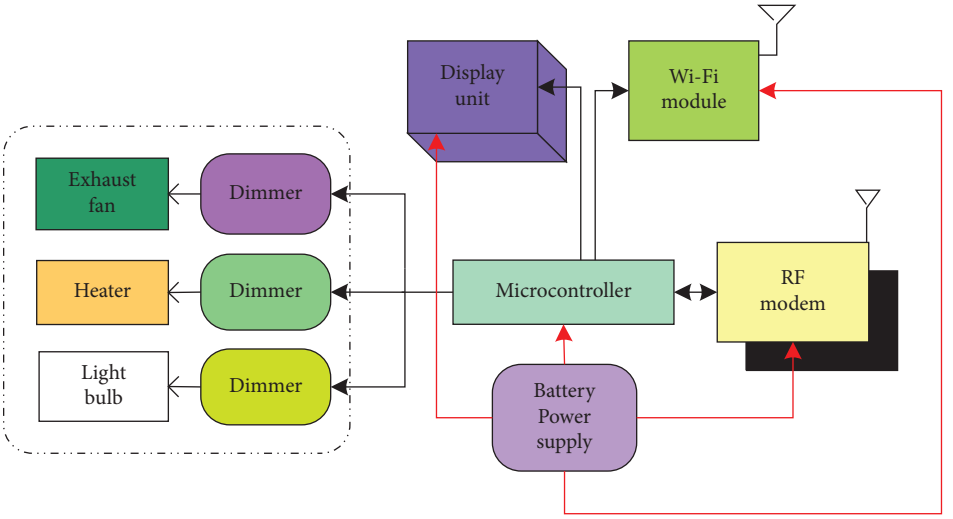

Figure 3: Block diagram of a receiver section.

mobile app is also utilized to control home appliances based on the environmental conditions of the home and the outer environment.

4. PID Controller with the Algorithm

The system is tuned to obtain the tuning parameters of PID with MATLAB Simulink, for a desired closed-loop response. The PID controller's system function is provided by the following equation:

$$G(s) = \mathbf{K_p} + \frac{\mathbf{K_i}}{\mathbf{S}} + \mathbf{k_d}^{\mathbf{s}}, \quad (1)$$

where K_p is the proportional gain, K_i is the integral gain, and K_d is the derivative gain.

The PID control system is optimized by adjusting certain performance indexes. The performance index is determined over a time interval "T." The performance indices [11] such as integral absolute error (IAE), integral square error (ISE), integral time absolute error (ITAE), and integral square time error (ISTE) are provided in the following equations:

$$\text{IAE} = \int_0^T e(t)dt, \quad (2)$$

$$\text{ISE} = \int_0^\infty e^2(t)dt, \quad (3)$$

$$\text{ITAE} = \int_0^T t|e(t)|dt, \quad (4)$$

$$\text{ISTE} = \int_0^T te^2(t)dt. \quad (5)$$

4.1. Optimization Algorithms. Many computing processes are required to achieve suitable matching factors for the system's derivation. To avoid computing complexity, many optimization approaches are applied. For finding the appropriate tuning settings, genetic algorithm (GA) and PSO algorithms have been considered for hardware-compatible optimization strategies.

4.1.1. Genetic Algorithm. GA is based on natural selection and genetic developmental theories, and it uses prior knowledge to route searches toward areas with greater search performance. Figure 4 shows the flow chart for the GA. The algorithm steps are as follows: initialization of the population of an individual, evaluation of fitness-by-fitness function, selection of fitness members of the population, application of mutation process, and best chromosome selection process when termination criteria are completed, so if not, search for another set of the best chromosomes.

Figure 5 represents the implementation of GA with the PID controller. A GA to determine the value of the PID controller's tuning parameters is called the GA-PID controller. The error signal is generated from the difference between the input value of the remote control and the feedback signal from the sensor. The device is connected to the controller via a dimming circuit. The height at which the trigger occurs is determined by the controller. GA helps to calculate optimized tuning parameters to control the PID controller, and the trigger level is determined based on the tuning parameter error signal.

4.1.2. PSO Algorithm. Eberhart and Kennedy suggested PSO in 1995. The birds' social behavior underlying the algorithm is the key notion. The particles travel at an initial speed according to the goal surface and attempt to change their speeds and locations on a local basis after each iteration. The steps involved in the PSO algorithm are as follows: enter all of the desired constraints, system functions, and PSO constants, as well as the number of particles. Set the particle positions and velocities to zero. Evaluate the system's fitness value with unit step response, calculate system constraints for each particle, and compare the individual fitness value of each particle to its previous value; if it is better than the previous one, replace it with a new value; otherwise do not change; the position of a particle with the lowest error is the global best value, particle position and velocity should be updated by equation (1), return to step 3, and repeat until all system constraints are met. Table 2 illustrates the parameters selected for the PSO algorithm and the equation for the optimization of parameters in the PSO algorithm.

Figure 6 shows PSO to find out the values for tuning parameters of the PID controller. The error signal is generated with the difference between the input value from the remote control and the feedback signal from the sensor.

5. Flow Diagram

In this section, we present the flow diagram of the semiautonomous mode, autonomous mode, and receiver.

5.1. Semiautonomous Mode. Figure 7 shows the flowchart, which discusses all the programming steps to develop the firmware of the remote control in semiautonomous mode, with embedded "C." The functions for liquid crystal display (LCD), universal synchronous and asynchronous receiver transmitter (USART), and analog-to-digital converter (ADC) are initialized. The controller waits for an interrupt signal after the remote control has been initialized.

When the interrupt signal is received, the user will have the option to select the mode of operation. If semiautonomous mode is selected, then values need to be predefined by the user through switches available on the remote control. After selecting the mode of operation, the controller will wait for another signal. Combinations of switches on the remote control are available for each appliance to select the device's dimming levels, and the signal generated by pressing the proper combination of switches will be processed through the controller. There are nine switches for the different functions of the controller. The "OK" switch is pressed to send the data in the form of a data packet with a unique ID to the receiver section. The same data are displayed on the LCD placed on the remote control.

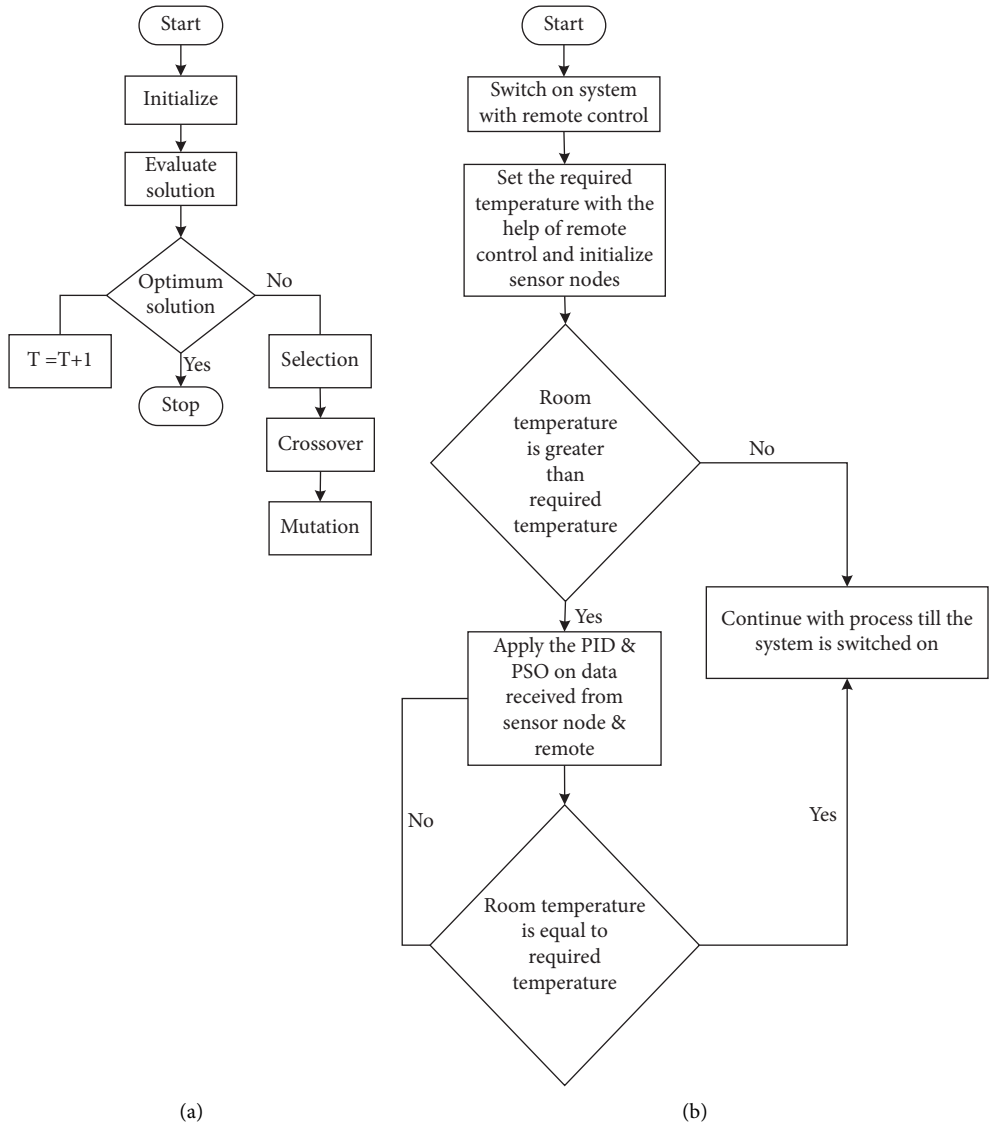

Figure 4: Flowchart for genetic algorithm (a). Flowchart for PSO algorithm (b).

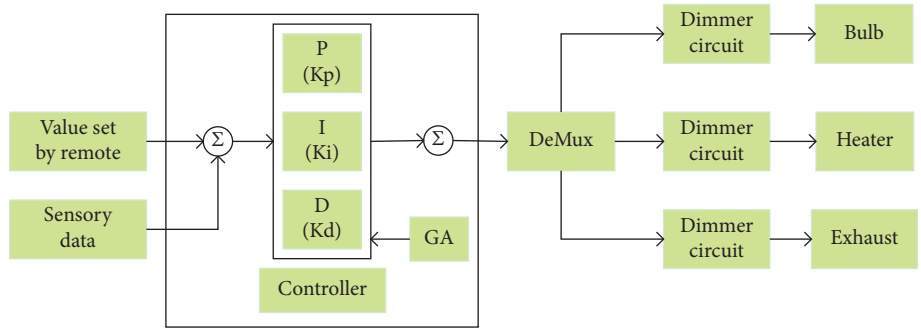

Figure 5: GA with PID controller for home appliance.

5.2. Autonomous Mode. Figure 8 shows the flowchart to discuss the steps involved in developing firmware for remote control in autonomous mode, with embedded "C" language. The functions for LCD, USART, and ADC are initialized. When the interrupt signal is received, the user will have the option of selecting the mode of operation. After the initialization of the receiver section, the controller waits for an interrupt signal. Here, remote control plays a significant role in the maintenance of ambient conditions in autonomous mode. The user must only supply physical parameter values

Table 2: Parameters selected in the PSO algorithm.

Parameters	Values
Number of birds (n)	40
Maximum number of birds	40
Dimension of the problem	2
PSO parameter c_1	1.3
PSO parameter c_2	0.14
PSO momentum or inertia (w)	0.9

The equation for optimization of parameters

Velocity = W ∗ velocity + $c_1 r_1$ ($l_{\text{best\_postion}}$ − c_position) + $c_2 r_2$ ($g_{\text{best\_postion}}$ − c_position)

W implies inertia weight; g_{best} implies global best; l_{best} implies local best; and r_1 and r_2 are random number;

c_position = c_position + velocity

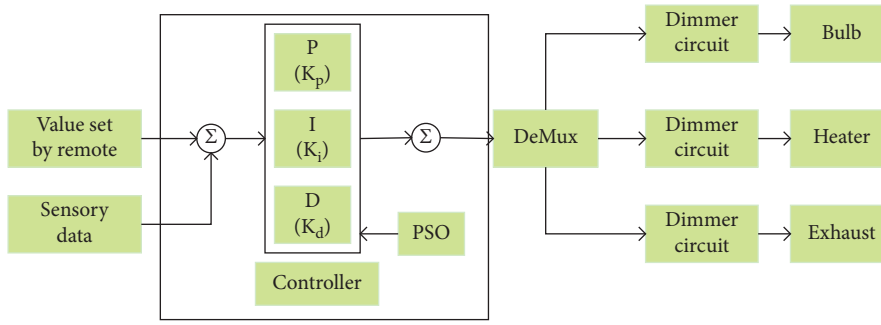

Figure 6: PSO with PID controller for home appliance.

like temperature, humidity, and light intensity via the switch array. The sensor value (signal-to-empty) measured by the user and input by the user (signal-to-empty section reference) is sent to the receiver section through a ZigBee packet.

5.3. Receiver. Figure 9(a) shows the interrupt subroutine, and Figure 9(b) shows the flowchart to discuss the steps involved in developing firmware for the receiver section, in embedded "C" language. In two separate modes, the recipient portion performs various functions. In semi-autonomous, the dimmer level of the appliance must only be determined by the settings specified by the user on the remote control. In stand-alone mode, however, the receiver generates an error signal by subtracting the sensor value from the remote-control input value. For the method employed with the PID controller, this error signal is used as an objective function. The PID, GA-PID, and PSO-PID values are calculated to calculate K_p, K_i, and K_d. The device is then activated at the required level by assessing the system's requirements for moving levels up and down. After selecting the appropriate dimming level, the appliance is to work on the directed voltage level. In the developed system, three appliances (heater, exhaust fan, and bulb) have been controlled.

6. Calibration of Sensors

The section describes the calibration of the sensors used for system development. The calibration and testing of sensors are done with the help of standard instruments, and results are verified. The dimming methodology is also discussed in detail, and power consumption for each level is calculated.

6.1. Temperature/Humidity Sensor. The temperature/humidity sensor is calibrated using a standard instrument called a psychrometer. It is necessary to use an intelligent system because, as time passes, the prior temperature rises. Once the system has reached the desired temperature, it must be lowered after some time to maintain a constant temperature. To analyze temperature and humidity level control for the system, a temperature/humidity sensor is used. The temperature/humidity sensor is connected in USART mode with a microcontroller. The values obtained for calibrating the humidity and temperature sensor are as presented in Table 3.

Figure 10(a) shows the comparison between relative humidity values given by the sensor and the standard instrument. Figure 10(b) shows that there is no error in the temperature value given by the sensor and standard instrument, as both values are overlapped. However, there is a slight difference between humidity values, which overcomes with the help of programming, and calibration for the temperature/humidity sensor is achieved accurately. After calibration, testing is also performed with standard instruments. For temperature testing, a thermometer is used, and for humidity testing, a humidity cabinet is used as shown in Figures 11(a) and 11(b).

6.2. LDR Sensor. The resistance of an LDR deviates from the sum of light that strikes it. The relationship between the light

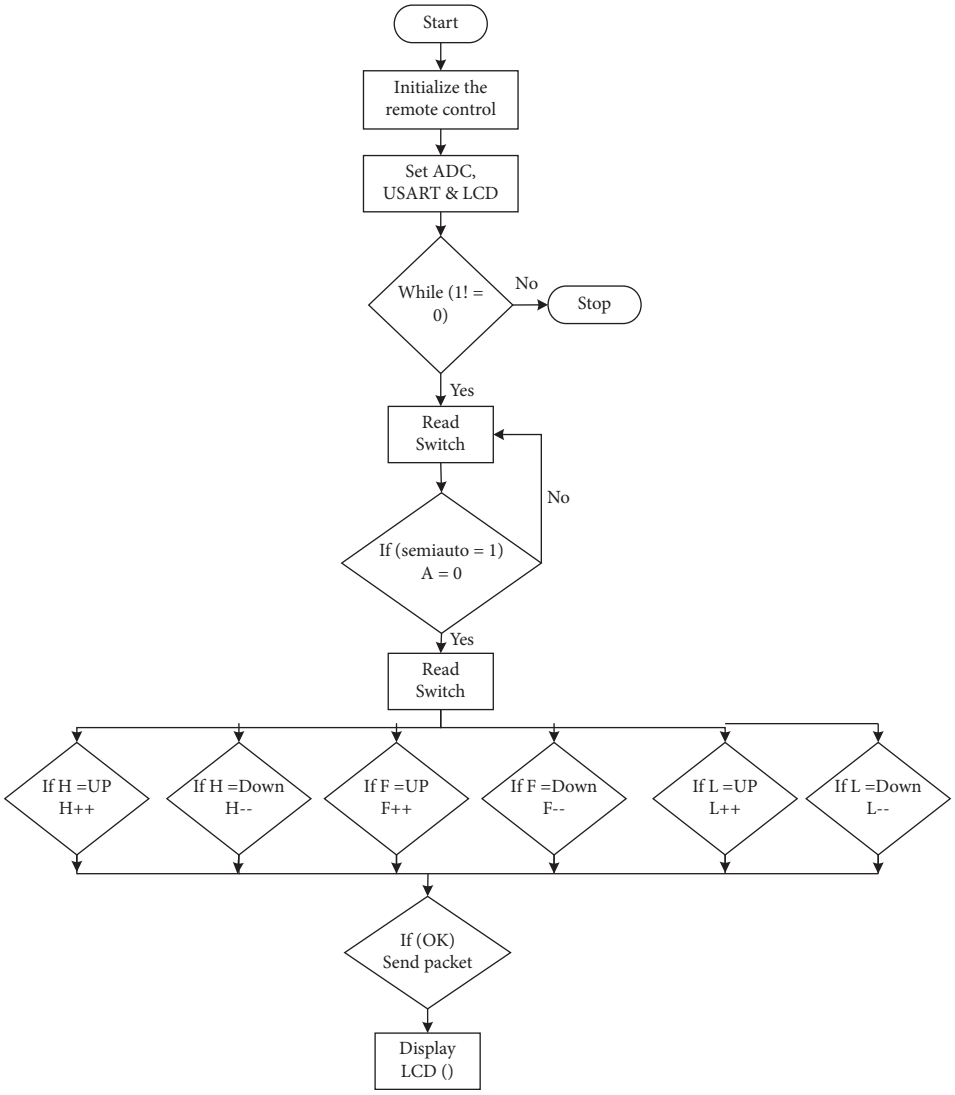

Figure 7: Flowchart for remote control in semiautonomous mode.

intensity lux for a typical LDR and load resistance (R_L) is as given in the following equation:

$$\mathbf{R_L} = \frac{\mathbf{500}}{\mathbf{Lux}} \text{ Kilo ohm.} \tag{6}$$

With the LDR connected to 5 V through a 10 K resistor, the output voltage of the LDR is as follows:

$$V_o = \frac{5 * R_L}{R_L + 10}. \tag{7}$$

Table 4 presents the values related to the relationship between resistance of LDR and with % illuminance level. The relationship between the resistance and light intensity is illustrated in Figure 12(a). LDR performance has been experimentally analyzed, and the result shows that calibration of the system is accurately achieved. Table 5 presents the values of the relation between lux and LDR % illuminance level. The relationship between the resistance values of LDR with the % illuminance level is presented in the table. Figure 12(b) shows the relation between the resistance values of LDR with the % illuminance level. The LDR gives the output as an analog signal, so it is connected to the ADC pin of a microcontroller.

6.3. Operation of Dimming System. In the dimmer circuit, the alternating current (AC) phase control method is used to control the intensity of the appliance. Concerning the firing angle of a triac, the RMS value of the voltage provided to the appliance is varied. The RMS voltage provided to the load changes as the firing angle is adjusted, and the voltage dimming level of the appliance is adjusted accordingly. The formula for firing angle calculation is expressed in the following equation:

$$\mathrm{V_o} = \frac{\mathrm{Vs}\sqrt{1/\pi\,(\pi - \alpha + (\sin 2\alpha))}}{2}, \tag{8}$$

where $\mathrm{V_o}$ is the RMS value of output voltage; $\mathrm{V_s}$ is the applied voltage; and α is the firing angle.

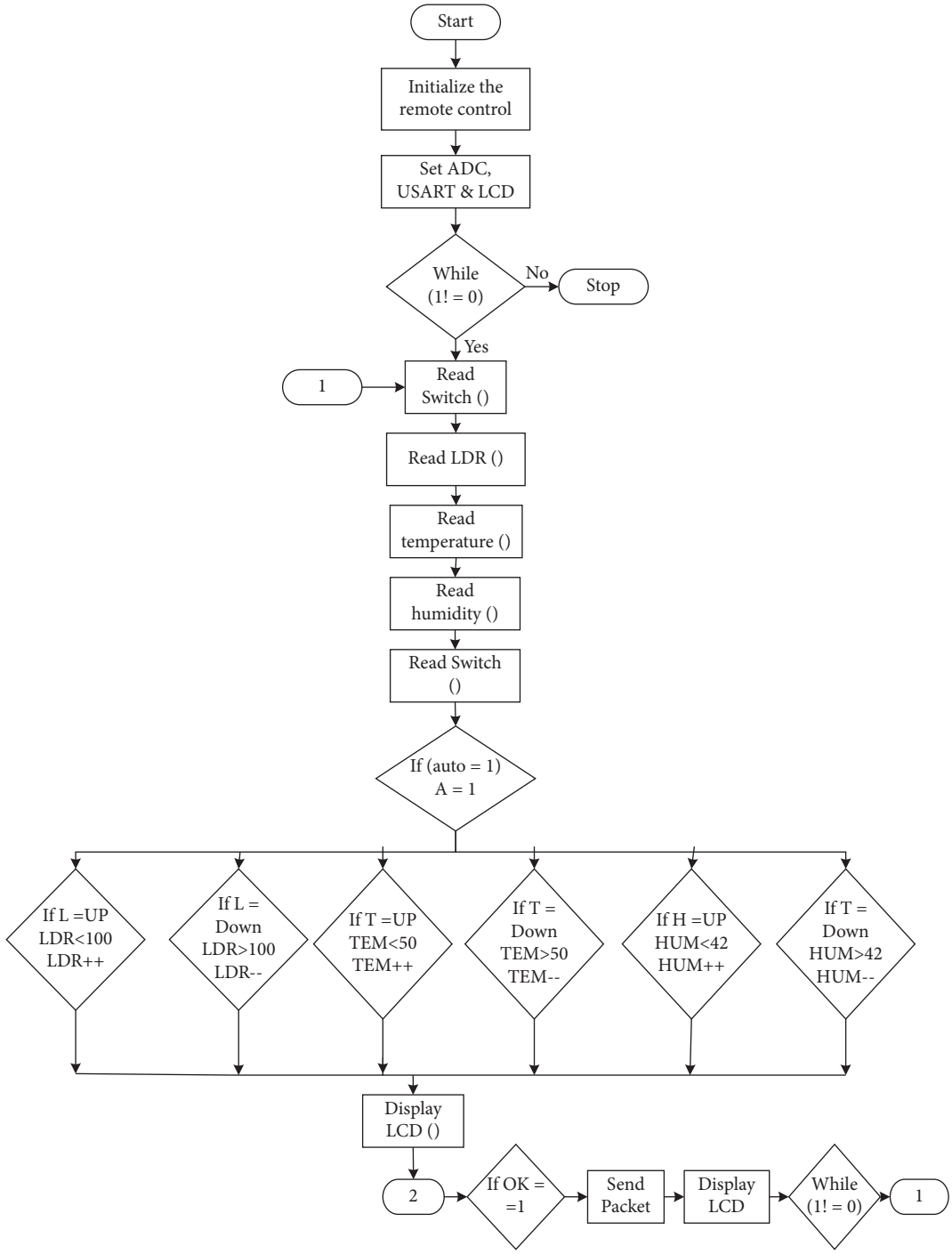

Figure 8: Flowchart for the remote section in autonomous mode.

From the formula given in equation (8), it is concluded that to control the dimming level of the appliance, triggering is required in different 16 levels as shown in Table 6. Figure 13 shows the variation in V_{rms} w.r.t firing angle and it can be observed that with an increase in firing angle, V_{rms} decreases.

According to firing angle and V_{rms} values for dimming levels, current is measured and the total power consumption is calculated. Table 7 shows the voltage, current, and power consumed by the bulb, exhaust fan, and heater at different dimming levels according to firing angle. It is observed that with an increase in level, the power consumption is also increasing, and appliances consume more power at higher levels.

Figure 14(a) illustrates the graph of the power consumption by 100 W bulb concerning dimming level. Figure 14(b) illustrates the graph of power consumption by 18 W exhaust fan concerning dimming level, and Figure 14(c) shows the power consumption by 1 KW heater for all the sixteen dimming levels.

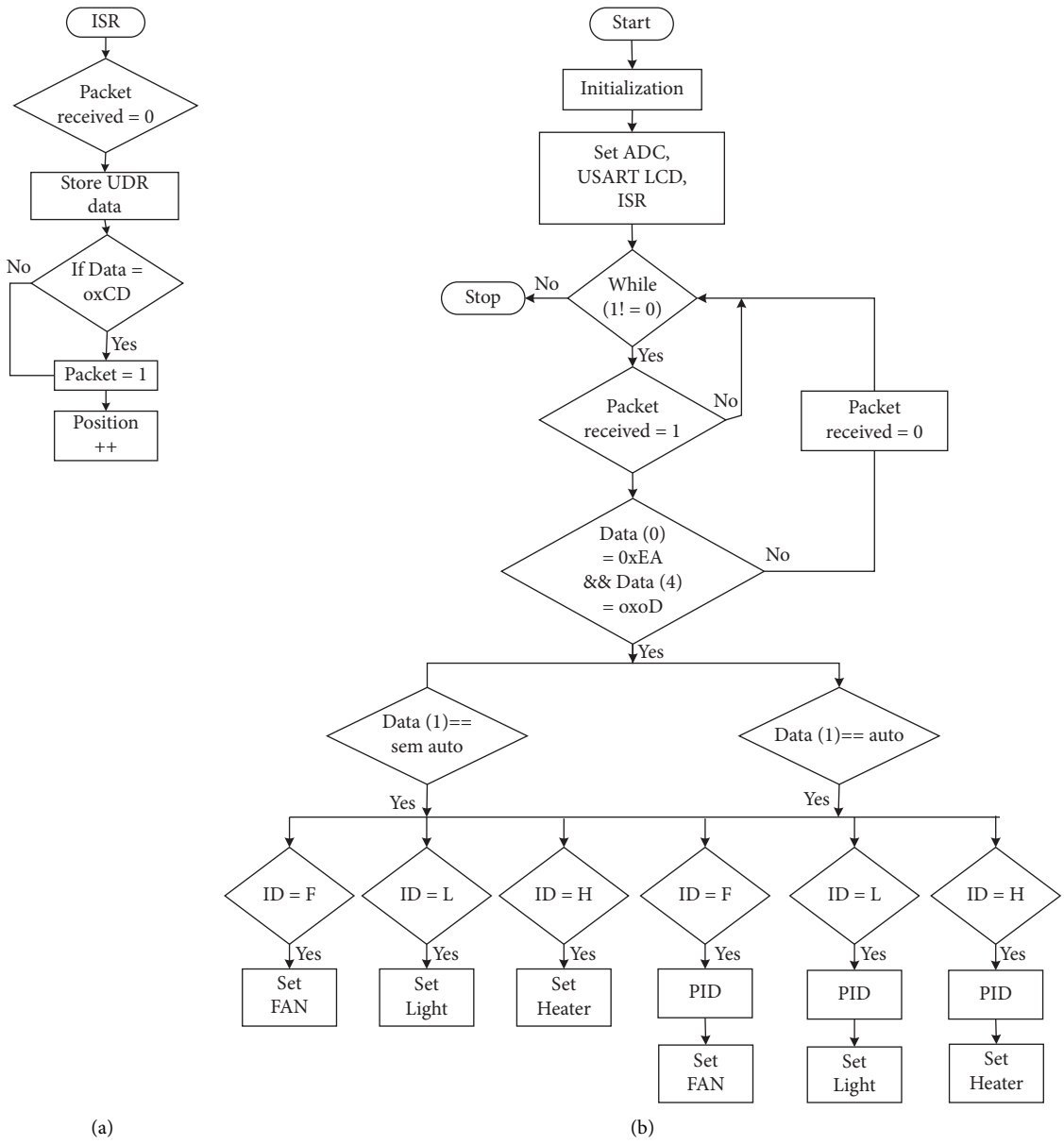

Figure 9: Flowchart for the receiver section (a). Flowchart for interrupt for the receiver section (b).

7. Results and Analysis

In this section, the experimental outcomes of the research are explained with the analysis for each appliance. Figures 15(a) and 15(b) present the receiver section, where there are three sockets on the board that correspond to the appliances such as the bulb, the heater, and the exhaust fan. The dimmer circuits are designed for controlling the light intensity, humidity, and temperature of the room. The system is tested in a room size of $10 * 8 * 10$ cubic feet, with a 100-Watt bulb, 1 KW room heater, and 18-Watt exhaust fan. In semiautonomous, dimming levels of appliances are controlled by setting the required level, with remote control as per the user's desire, and remote control in the semiautonomous mode is shown in Figure 15(c). In the autonomous mode, the dimming level is controlled by an error signal generated from the difference between sensors of the remote control. The input value of the parameter set by the user and the remote control in the autonomous mode is shown in Figure 15(d). The sensors are calibrated with standard instruments before implementation on the system. The standard instrument for light intensity is a lux meter, and for humidity and temperature, the psychrometer is used.

Table 3: Humidity and temperature from standard instruments and sensors.

Time	Dry temperature by standard instrument (in °C)	Wet temperature by standard instrument (in °C)	Temperature by sensor (in °C)	Temperature errors (%)	Relative humidity by standard instrument (%)	Relative humidity by sensor (%)	Humidity errors (%)
9:30 AM	20	12.1	20	0	44.8	45	−0.004
10:00 AM	21	12.7	21	0	43.6	44	−0.009
10:30 AM	22	13.4	22	0	43.1	43	0.0023
11:00 AM	23	13.8	23	0	41	41	0
11:30 AM	24	14.1	24	0	41.6	42	−0.009
12:00 PM	25	15.1	25	0	40	40	0
12:30 PM	26	16.1	26	0	40.7	41	−0.007
1:00 PM	27	16.5	27	0	39	39	0
1:30 PM	28	17.1	28	0	38.2	38	0.0052

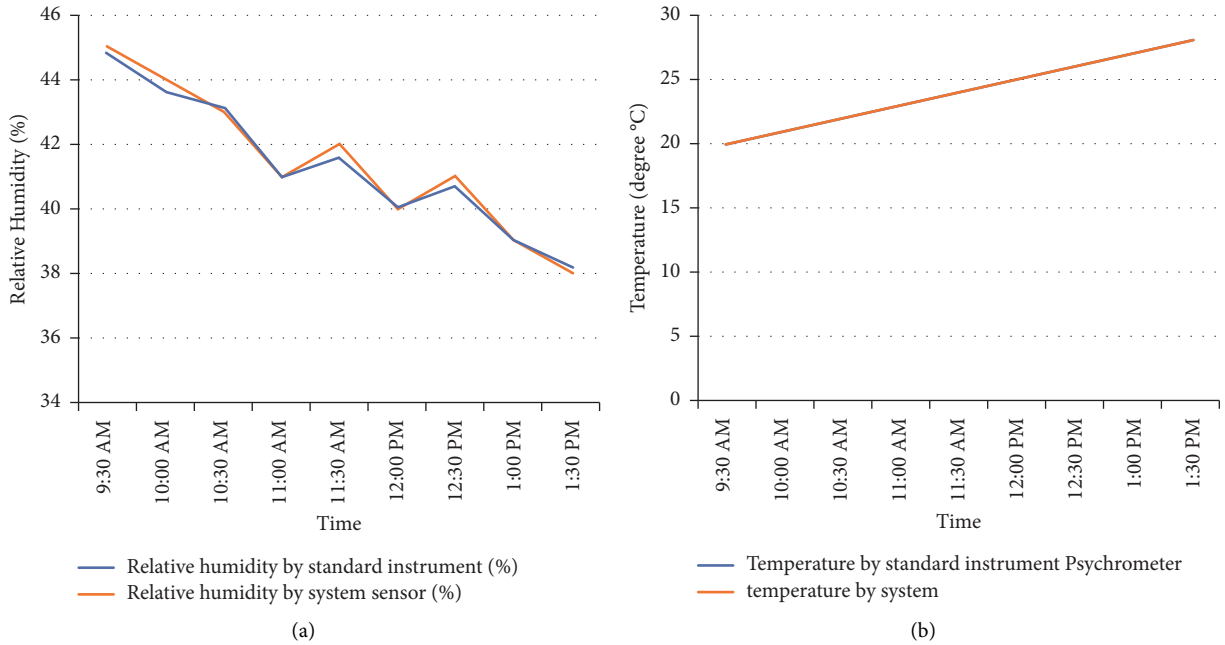

Figure 10: (a) Relative humidity values by the sensor and standard instrument. (b) Relative temperature values by the sensor and standard instrument.

(a) (b)

Figure 11: (a) Testing of a temperature sensor with a standard thermometer. (b) Testing of humidity sensor with a standard instrument.

The results are analyzed in terms of percentage saving of power w.r.t conventional appliances. The experimental outcomes of the heater, bulb, and exhaust fan are presented by implementing three different techniques, namely, PID, GA-PID, and PSO-PSD.

7.1. Experiment Outcomes for Heater. The tuning parameters are calculated for all three methods with the MATLAB tool using PID, GA-PID, and PSO-PID. An experiment is conducted in a room size of $10 * 8 * 10$, and the performance of every appliance is analyzed individually. As per the standards, a 1 KW heater is sufficient for this size of the room. The experiment is carried out with 1 KW in a room size of $10 \times 8 \times 10$ in March 2020, for two hours, with the initial temperature observed as 29°C. The target is to maintain the room temperature at 30°C.

Figure 16 shows the power consumption of the heater during the experimental period; during the first 30 minutes, all methods use the same power as the system to reach the set temperature value. It is observed that in half an hour (8:30 A.M to 9:00 A.M), there is a 1°C of temperature rise, as the target was to maintain 30°C with 29°C initial temperature. So, the system consumed the same power as the conventional heater. After reaching a set value of temperature, the temperature starts increasing due to the effect of the external environment. To nullify this effect, the system is triggered at the lower level. Now, the temperature drops, and to maintain a required level, the system is triggered at a higher level.

Power analysis is performed using PID, GA-PID, and PSO-PID to keep the heater power consumption at a temperature of 300°C and the initial temperature at 29°C. It is concluded that power consumption by the conventional heater is 1.8 KW for two hours. Power consumption by the heater with PID controller is 1.703 KW, with GA-PID it is 1.605 KW, and with PSO-PIS it is 1.532 KW. The power saving w.r.t conventional heater is calculated in each case, and it is shown

Table 4: Relation between resistance values of LDR with % illuminance level.

Illuminance levels (%)	R (K ohm)
0	18
10	12.9
20	10.7
30	9.8
40	7.5
50	5.5
60	3.9
70	2.4
80	1.9
90	0.5
100	0

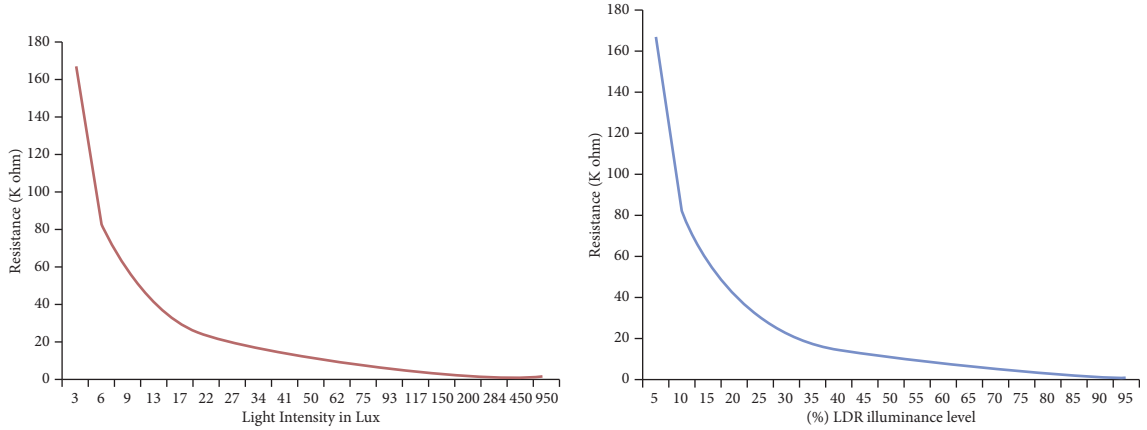

Figure 12: (a) Relation between resistance (K ohm) of light intensity in lux. (b) Relation between resistance (K ohm) of LDR with % illuminance level.

Table 5: Relation between lux and LDR % illuminance level.

Illuminance of LDR (%)	Light intensity (lux)
0	0
10	6
20	13
30	22
40	34
50	50
60	75
70	117
80	200
90	450

in Table 8. Figure 17 shows that the power efficiency for PID is 5.38%, for GA-PID it is 10.83%, and for PSO-PID it is 14.88%. Results clearly show that PSO-PID consumes less power than PID and GA-PID and is the best suited for the designed system.

7.2. Experiment Outcomes for Bulb. For bulb analysis, the values of PID parameters Kp, Ki, and Kd are tuned with PID, GA-PID, and PSO-PID. An experiment is conducted in a room size of $10 * 8 * 10$ with 100 W, in March 2020 at home. An experiment is performed for four hours, with

Table 6: Relation between firing angles and V_{rms} w.r.t α.

Dimming levels	Firing angles (α) in degree	V_{rms} (V)
0	180	0
1	175	2
2	167	10
3	159	22
4	149	39
5	140	55
6	132	72
7	123	89
8	113	110
9	105	126
10	95	145
11	85	163
12	83	167
13	74	180
14	62	195
15	7	220

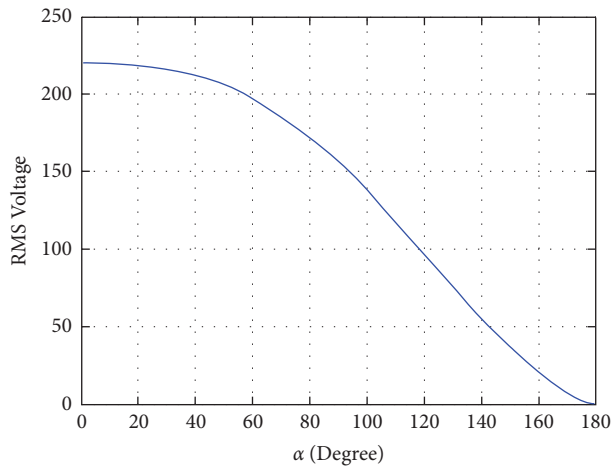

Figure 13: Variation of V_{rms} w.r.t firing angle.

Table 7: Power consumed by the heater, bulb, and fan.

Dimming levels	Firing angles	Voltage (V)	Current (mA) for bulb	Current (mA) for heater	Current (mA) for exhaust	Power consumption by 100 W bulb (W)	Power consumption by 1 KW heater (W)	Power consumption by 18 W exhaust (W)
0	180	0	0	0	0	0	0	0
1	175	2	4	38	0	0.008	0.076	0
2	167	10	20	192	0	0.2	1.92	0
3	159	22	45	423	8	0.99	9.306	0.176
4	149	39	80	750	14	3.12	29.25	0.546
5	140	55	113	1058	20	6.215	58.19	1.1
6	132	72	149	1385	26	10.728	99.72	1.872
7	123	89	184	1170	32	16.376	104.13	2.848
8	113	110	227	2110	40	24.97	232.1	4.4
9	105	126	260	2423	46	32.76	305.29	5.796
10	95	145	300	2780	53	43.5	403.1	7.685
11	85	163	337	3130	60	54.931	510.19	9.78
12	83	167	345	3210	61	57.615	536.07	10.187
13	74	180	351	3269	62	63.18	588.42	11.16
14	62	195	358	3327	63	69.81	648.76	12.285
15	7	220	455	4347	81	100	956.34	17.82

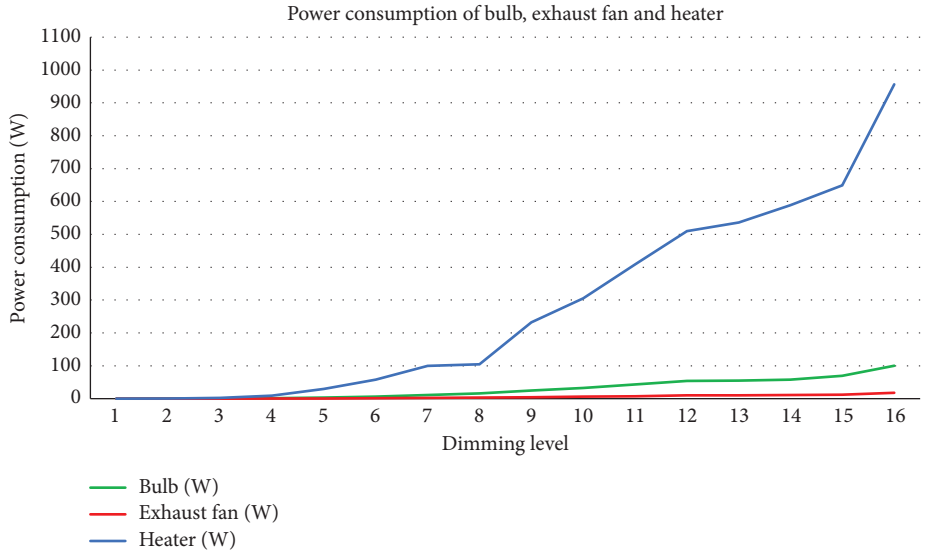

Figure 14: Power consumed by 100 W bulb, 18 W fan, and heater.

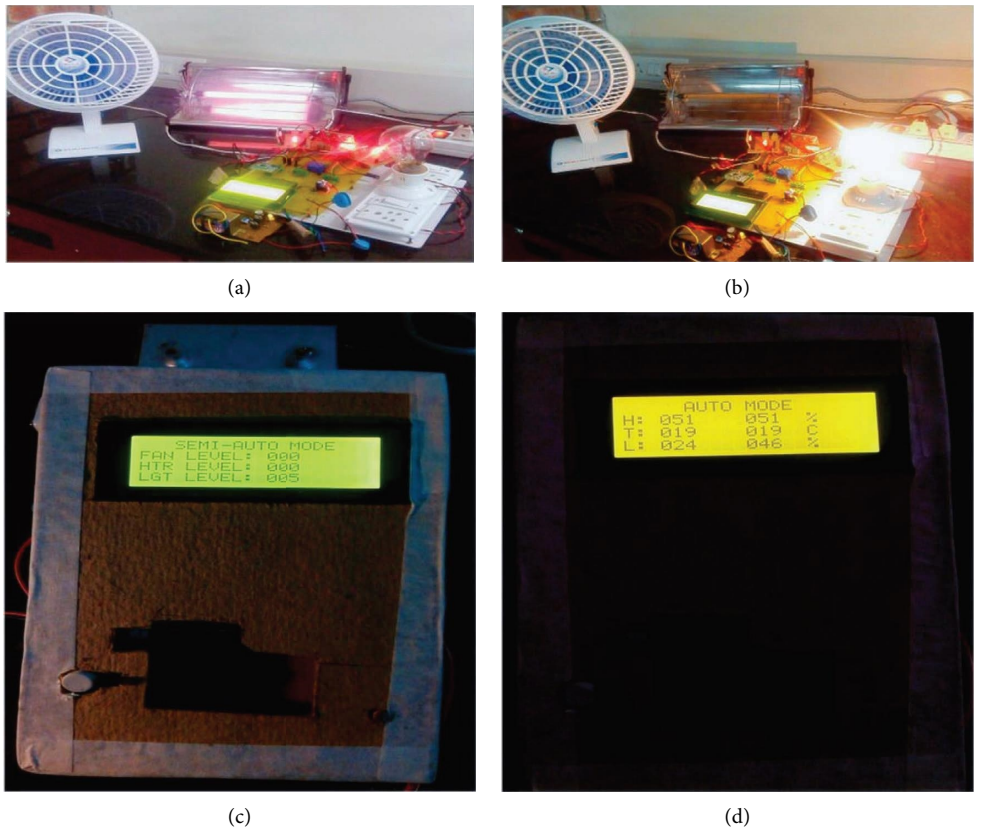

Figure 15: Hardware implementation of receiver and remote control in real-time. (a) Hardware of receiver section switching on heater and exhaust fan. (b) Hardware of receiver section switching on bulb and exhaust fan. (c) Remote control device in operating in semiauto mode. (d) Remote control device in operating in auto mode.

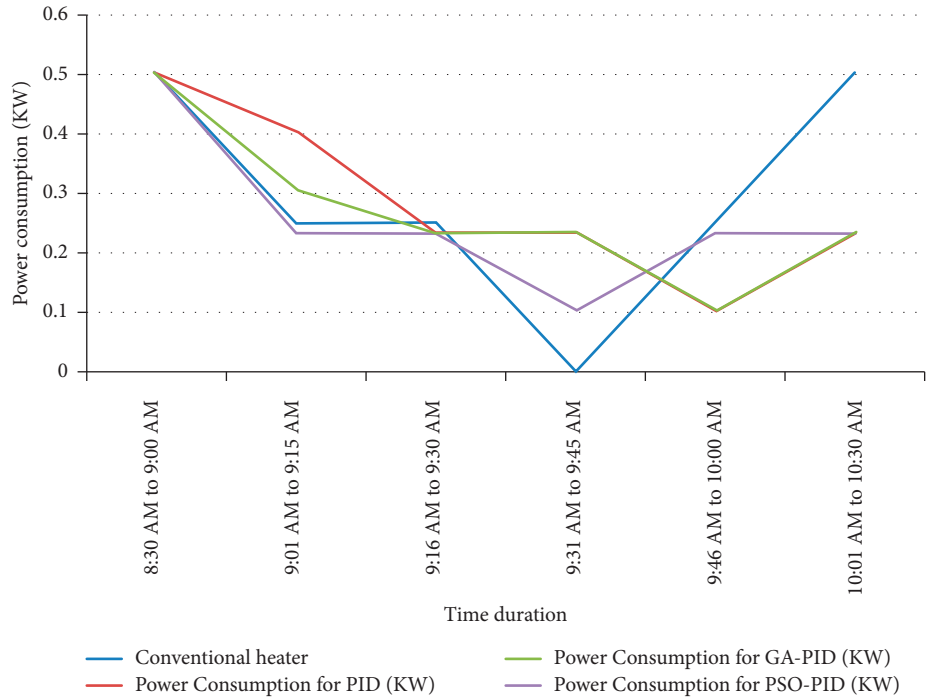

Figure 16: Power consumption for the heater in (KW) for PID, GA-PID, and PSO-PID during the experiment.

a background light intensity of 20 lux. The values from lux meter are in lux and from LDR in %. The target was to maintain the light intensity at 80%. PID, PSO-PID, and GA-PID are used to analyze the power usage of a 100 W bulb to keep the light intensity at 200 lux or 80 percent LDR with 20 percent initial intensity.

The energy meter power consumption is calculated and presented in Figure 18. It is concluded that power consumption by the conventional bulb is 400 W for four hours (with the assumption, it is switched off at 10:30 P.M). Power consumption with PID controller is 278.7 W, with GA-PID it is 253.1 W, and with PSO-PIS it is 250.02 W. The power saving w.r.t the conventional bulb was observed in each case. Figure 19 shows that the power saving for PID is 30%, for GA-PID saving is 37%, and for PSO-PID it is 37.49%. Results in Table 9 show that the PSO-PID method consumes less power than PID and GA-PID and it is best suited for the designed system.

7.3. Experiment Outcomes for Exhaust Fan. For exhaust fan analysis, the values of PID tuning parameters Kp, Ki, and Kd are tuned with PID, GA-PID, and PSO-PID. The tuning parameters are calculated for all three methods. The experiment is conducted in a room size of $10 * 8 * 10$ with an 18 W exhaust fan, in March 2020. Experiment data are collected for four hours, with initial humidity of 44%. The target is to maintain the humidity at 42%. Based on readings taken with the energy meter; power is calculated and presented in Figure 20. Moreover, it is concluded that power consumption by a conventional exhaust fan is 72 W for four hours. Power consumption by exhaust with PID controller is 48.9 W, with GA-PID it is 47.5 W, and with PSO-PID it is 45.4 W.

Figure 21 shows that % of power saving for PSO-PID is 36.9%, PID is 32%, and GA-PID is 34%. Results in Table 10 clearly show that PSO-PID consumes less power than PID and GA-PID and is best suited for the designed system.

7.4. Current Consumption Analysis. In this section, we discuss the current consumption by receiver section and remote control in detail. Tables 11 and 12 show current consumption for both the remote control and receiver section in mA. Remote control consumes 99.5 mA of current, and the receiver section consumes 154 mA of

Table 8: % of power saving w.r.t conventional heater.

Power consumption by a conventional heater (KW)	Power consumption by using PID controller (KW)	Power consumption by using GA-PID controller (KW)	Power consumption by using PSO-PID controller (KW)	Power saving by using PID controller (%)	% power saving by using GA-PID controller (%)	% power saving by using PSO-PID controller (%)
1.8	1.703	1.605	1.532	5.38	10.83	14.88

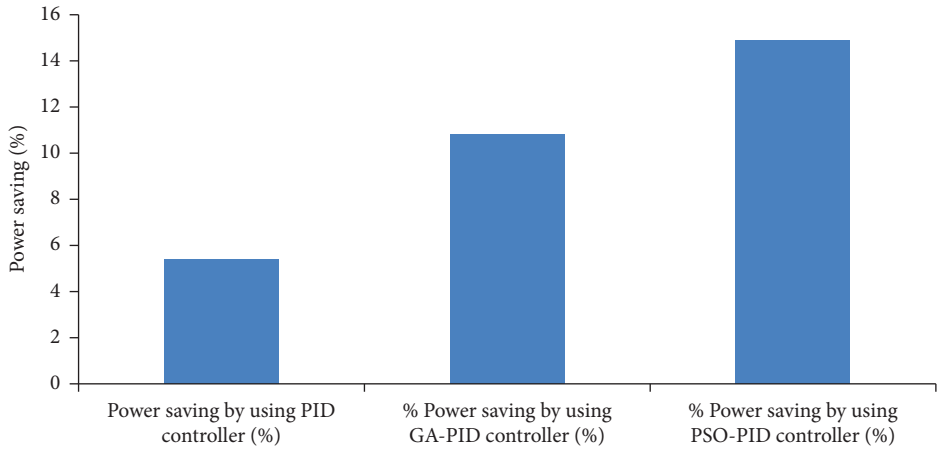

Figure 17: Power saving (%) w.r.t conventional heater.

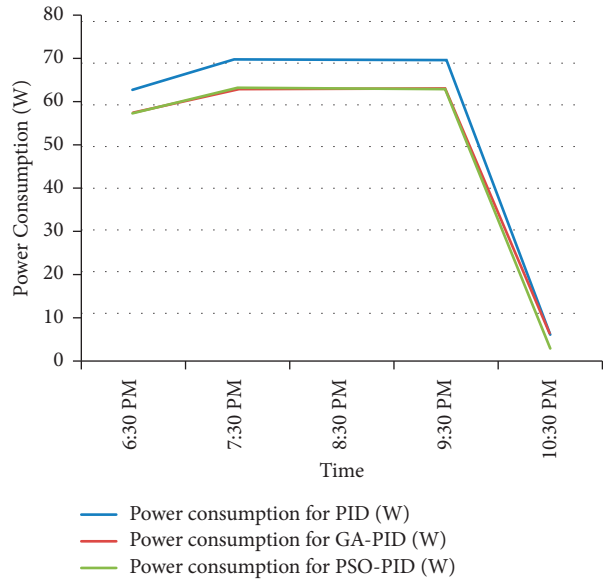

Figure 18: Power consumption for the bulb in (W) for GA-PID, PID, and PSO-PID during the experiment.

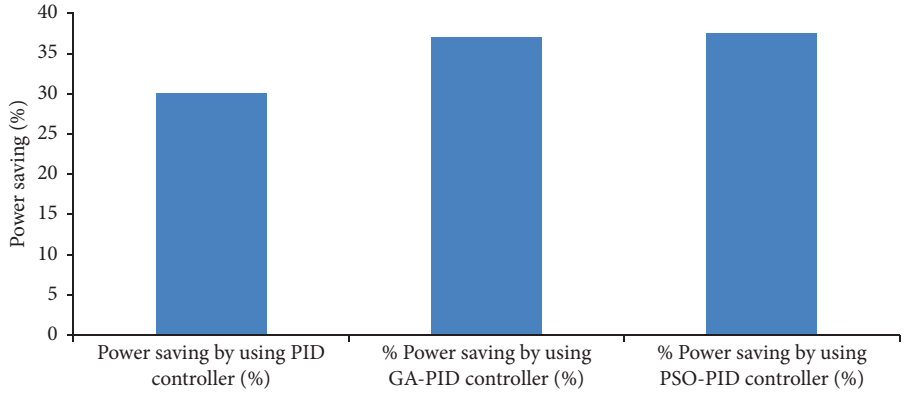

Figure 19: Power saving w.r.t conventional bulb.

Table 9: % of saving power w.r.t bulb (100 W) for the four hours.

Power consumption by a conventional bulb (W)	Power consumption by using PID controller (W)	Power consumption by using GA-PID controller (W)	Power consumption by using PSO-PID controller (W)	Power saving by using PID controller (%)	% power saving by using GA-PID controller (%)	% power saving by using PSO-PID controller (%)
400	278.7	253.1	250.02	30	37	37.49

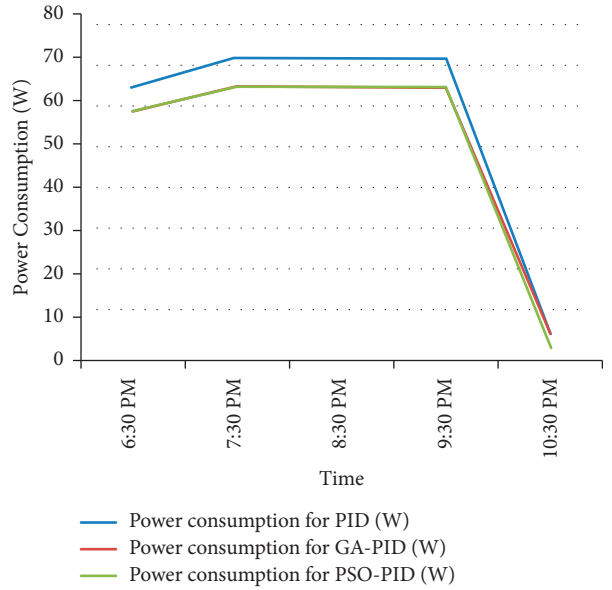

Figure 20: Power consumption for exhaust fan in (W) for PID, GA-PID, and PSO-PID.

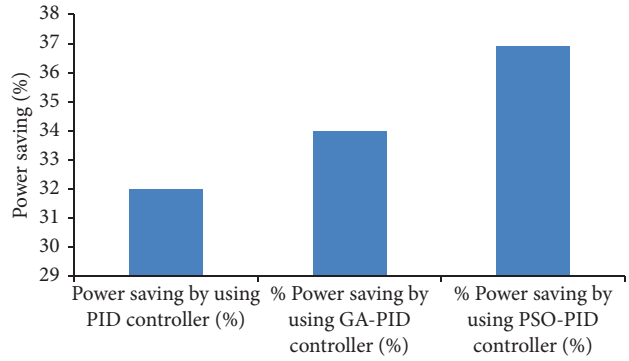

Figure 21: % of saving power of exhaust fan.

current. Even though power was not a design issue for the system, it is evident that the designed system requires very little power.

The total power consumption by remote control comes out as (99.5 mA ∗ 5 V = 497.5 mW); the three components that dominate power consumption for remote control are the microcontroller, RF modem, and temperature/humidity sensor. The battery used in this application is a rechargeable lithium-ion battery with a potential of 12 V/1 A; thus, it can be used continuously (day/night) in the application for approximately 25 days. The receiver section is to be fitted with switchboards, so it

Table 10: % of saving power of exhaust fan (18 W) for four hours.

Power consumption by the conventional exhaust fan (W)	Power consumption by using PID controller (W)	Power consumption by using GA-PID controller (W)	Power consumption by using PSO-PID controller (W)	Power saving by using PID controller (%)	% power saving by using GA-PID controller (%)	% power saving by using PSO-PID controller (%)
72	48.9	47.5	45.4	32	34	36.9

Table 11: Consumption of current for remote control.

Modules	Current consumption (mA)
ATmega 16	17
Temperature/humidity sensor	20
LDR	0.5
RF modem	58
LCD (20 × 4)	4
Total	**99.5**

The bold is made to show the total value of current in Table 11.

Table 12: Consumption of current for remote control.

Components	Current consumptions (mA)
ATmega 16	17
Three dimmers	25 × 3 = 75
RF modem	58
LCD (20 × 4)	4
Total	**154**

The bold is made to show the total value of current in Table 12.

takes power from the main supply through the regulator. The total current consumption by receiver section is shown in Table 12 and comes out to 154 mA.

8. Conclusion

The concern of electricity scarcity is prevalent due to the expansion of population growth. Smart devices are being widely implemented in the home to reduce power usage in home appliances owing to power shortages. However, there is still a lack of research that implements optimization techniques with remote controllers to reduce energy consumption in homes. To overcome these challenges, this study proposed a system that operates in autonomous and semiautonomous modes to control home appliances according to environmental conditions. Of the MATLAB analysis, PID-PSO algorithm is concluded as optimal to control the home appliance under suitable environmental conditions. Finally, from the experimental results, the PSO-PID controller delivered an energy saving of 14.88% for the heater, 36.9% for the exhaust fan, and 37.49% for the light bulb compared to the conventional appliances. A 2.4 GHz RF module is used to establish wireless personal network communication between the remote and the receiver. A Wi-Fi modem is integrated with the receiver to activate the control of appliances through the mobile application based on the Internet.

Data Availability

Data available on request from the authors.

Conflicts of Interest

The authors declare that they have no conflicts of interest.

References

[1] Enerdata, "Electricity Production Data World Electricity Statistics," 2021, https://yearbook.enerdata.net/electricity/world-electricity-production-statistics.html.

[2] Enerdata, "World Power Consumption Electricity consumption," 2021, https://yearbook.enerdata.net/electricity/electricity-domestic-consumption-data.html.

[3] M. Moyeed Abrar, "Power cut off and power blackout in India a major threat- an overview," *International Journal of Advanced Research and Technology*, vol. 5, pp. 8–15, 2016.

[4] D. Gielen, F. Boshell, D. Saygin, M. D. Bazilian, N. Wagner, and R. Gorini, "The role of renewable energy in the global energy transformation," *Energy Strategy Reviews*, vol. 24, pp. 38–50, 2019.

[5] S. Scharl and A. Praktiknjo, "The role of a digital industry 4.0 in a renewable energy system," *International Journal of Energy Research*, vol. 43, no. 8, pp. 3891–3904, 2019.

[6] W. A. Jabbar, M. H. Alsibai, N. S. S. Amran, and S. K. Mahayadin, "Design and implementation of IoT-based automation system for smart home," in *Proceedings of the 2018 International Symposium on Networks, Computers and Communications (ISNCC)*, pp. 1–6, IEEE, Rome, Italy, June 2018.

[7] J. Iqbal, M. Ullah, S. G. Khan, B. Khelifa, and S. Ćuković, "Nonlinear control systems-A brief overview of historical and recent advances," *Nonlinear Engineering*, vol. 6, no. 4, pp. 301–312, 2017.

[8] P. H. Shaikh, N. B. M. Nor, P. Nallagownden, I. Elamvazuthi, and T. Ibrahim, "A review on optimized control systems for building energy and comfort management of smart sustainable buildings," *Renewable and Sustainable Energy Reviews*, vol. 34, pp. 409–429, 2014.

[9] N. Nalajala, H. Chen, and T. Jin, "A closed-loop home energy automation system via power provisioning," in *Proceedings of the 2013 IEEE International Conference on Cyber Technology In Automation, Control and Intelligent Systems*, pp. 423–427, IEEE, Nanjing, China, May 2013.

[10] R. Ford, M. Pritoni, A. Sanguinetti, and B. Karlin, "Categories and functionality of smart home technology for energy management," *Building and environment*, vol. 123, pp. 543–554, 2017.

[11] N. Shet and S. Chokkadi, "Home automation Indian scenario: a survey of architectures and technologies," *International Journal of Scientific Engineering and Research*, vol. 3, no. 4, 2012.

[12] A. Kanungo, M. Mittal, and L. Dewan, "Wavelet based PID controller using GA optimization and scheduling for feedback systems," *Journal of Interdisciplinary Mathematics*, vol. 23, no. 1, pp. 145–152, 2020.

[13] M. A. Ramya, S. P. Jadhav, and S. N. Pawar, "Design and implementation of particle swarm optimization (PSO) tuned PID controller for speed control of permanent magnet brush less DC (PMBLDC) motor," in *Proceedings of the 2020 International Conference for Emerging Technology (INCET)*, pp. 1–6, IEEE, Belgaum, India, June 2020.

[14] M. El-Abd, "Performance assessment of foraging algorithms vs. evolutionary algorithms," *Information Sciences*, vol. 182, no. 1, pp. 243–263, 2012.

[15] J. Kim, C. H. O. I. Yunho, L. E. E. Chongho, and D. Chung, "Implementation of a high-performance genetic algorithm processor for hardware optimization," *IEICE - Transactions on Electronics*, vol. 85, no. 1, pp. 195–203, 2002.

[16] S. Sun, K. Y. Kim, O. S. Shin, and Y. Shin, "Device-to-device resource allocation in LTE-advanced networks by hybrid particle swarm optimization and genetic algorithm," *Peer-to-Peer Networking and Applications*, vol. 9, no. 5, pp. 945–954, 2016.

[17] I. Damaj, M. Elshafei, M. El-Abd, and M. E. Aydin, "An analytical framework for high-speed hardware particle swarm optimization," *Microprocessors and Microsystems*, vol. 72, Article ID 102949, 2020.

[18] K. L. Ku, J. S. Liaw, M. Y. Tsai, and T. S. Liu, "Automatic control system for thermal comfort based on predicted mean vote and energy saving," *IEEE Transactions on Automation Science and Engineering*, vol. 12, no. 1, pp. 378–383, 2015.

[19] Z. Y. Liu, "Hardware design of smart home system based on ZigBee wireless sensor network," *AasriProcedia*, vol. 8, pp. 75–81, 2014.

[20] H. Ramezanian, S. Balochian, and A. Zare, "Design of optimal fractional-order PID controllers using particle swarm optimization algorithm for automatic voltage regulator (AVR) system," *J. Control. Autom. Electr. Syst.* vol. 24, no. 5, pp. 601–611, 2013.

[21] K.-H. Teng, Z.-Y. Lam, and S.-K. Wong, "Dimmable WiFi-connected LED driver with android based remote control," in *Proceedings of the 2013 IEEE Symposium on Wireless Technology & Applications (ISWTA)*, pp. 306–309, IEEE, Kuching, Malaysia, September 2013.

[22] R. Zhang and L. Gao, "Research on motor control and simulation based on PID and Internet of Things system," *Microprocessors and Microsystems*, vol. 80, Article ID 103602, 2021.

[23] I. Chiha, N. Liouane, and P. Borne, "Tuning PID controller using multiobjective ant colony optimization," *Applied Computational Intelligence and Soft Computing*, vol. 2012, Article ID 536326, 7 pages, 2012.

[24] N. Javaid, I. Khan, M. N. Ullah, A. Mahmood, and M. U. Farooq, "A survey of home energy management systems in future smart grid communications," in *Proceedings of the 2013 Eighth International Conference on Broadband and Wireless Computing, Communication and Applications*, pp. 459–464, IEEE, Compiegne, France, October 2013.

[25] W. Huang and H. N. Lam, "Using genetic algorithms to optimize controller parameters for HVAC systems," *Energy and Buildings*, vol. 26, no. 3, pp. 277–282, 1997.

[26] D. H. Kim and J. I. Park, "Intelligent PID controller tuning of AVR system using GA and PSO," in *Proceedings of the International Conference on Intelligent Computing*, pp. 366–375, Springer, Berlin, Heidelberg, August 2005.

[27] S. Park, M. I. Choi, B. Kang, and S. Park, "Design and implementation of smart energy management system for reducing power consumption using ZigBee wireless communication module," *Procedia Computer Science*, vol. 19, pp. 662–668, 2013.

[28] S.-C. Wang, Y.-L. Chen, H.-B. Lin, K.-Y. Shen, and K.-C. Huang, "Realization of a high-efficiency T5 ballast with multi-dimming mechanisms based on lamp arc modeling," in *Proceedings of the 2013 IEEE 8th Conference on Industrial Electronics and Applications (ICIEA)*, pp. 1077–1082, IEEE, Melbourne, VIC, Australia, June 2013.

[29] C. Li, K. Dong, F. Jin, J. Song, and W. Mo, "Design of smart home monitoring and control system based on Zigbee and WIFI," in *Proceedings of the 2016 International Conference on Robots & Intelligent System (ICRIS)*, pp. 6345–6348, IEEE, ZhangJiaJie, China, August 2019.

[30] A. A. Lukman, J. Agajo, K. J. Gana, I. C. Ogbole, and E. E. Ataimo, "Development of a low power consumption smart embedded wireless sensor network for the ubiquitous environmental monitoring using ZigBee module," *ATBU Journal of Science Technology and Education.*vol. 5, pp. 94–108, 2017.

[31] Y. M. Yusoff, R. Rosli, M. U. Karnaluddin, and M. Samad, "Towards smart street lighting system in Malaysia," in *Proceedings of the 2013 IEEE Symposium on Wireless Technology & Applications (ISWTA)*, pp. 301–305, IEEE, Kuching, Malaysia, September 2013.

[32] Y. W. Lin, Y. B. Lin, C. Y. Hsiao, Y. Y. Wang, and R. C. IoTtalk, "IoTtalk-RC: sensors as universal remote control for aftermarket home appliances," *IEEE Internet of Things Journal*, vol. 4, pp. 1104–1112, 2017.

[33] Y. N. Lin, S. K. Wang, C. Y. Yang, V. R. L. Shen, T. T. Y. Juang, and W.-H. Hung, "Development and verification of a smart remote control system for home appliances," *Computers & Electrical Engineering*, vol. 88, Article ID 106889, 2020.

[34] H. Tanaka, H. Suzuki, A. Watanabe, and K. Naito, "Evaluation of a secure end-to-end remote control system for smart home appliances," in *Proceedings of the 2018 IEEE International Conference on Consumer Electronics (ICCE)*, pp. 1-2, IEEE, Las Vegas, NV, USA, January 2018.

[35] F. E. Sandnes, J. Herstad, A. M. Stangeland, and F. O. Medola, "UbiWheel: a simple context-aware universal control concept for smart home appliances that encourages active living," in *Proceedings of the 2017 IEEE SmartWorld, Ubiquitous Intelligence & Computing, Advanced & Trusted Computed, Scalable Computing & Communications, Cloud & Big Data Computing, Internet of People and Smart City Innovation (SmartWorld/SCALCOM/UIC/ATC/CBDCom/IOP/SCI)*, pp. 1–6, IEEE, San Francisco, CA, USA, August 2017.

[36] D. K. Amesimenu, K.-C. Chang, T.-W. Sung et al., "Home appliances control using android and arduino via bluetooth and GSM control," in *Proceedings of the International Conference on Artificial Intelligence and Computer Vision (AICV2020). AICV 2020*, pp. 819–827, Springer, Cairo, Egypt, April 2020.

[37] P. K. T. Campus and P. K. T. Campus, "IoT Based Universal Remote Controller for Smart Home Environment," *Internationaljournalfor Innovative Research In Multidisciplinary Field*, vol. 3, pp. 78–85, 2017.

[38] W. H. Lee, C.-M. Chou, and W. C. Chen, "Design and implementation of an NFC-based universal touch and control platform," in *Proceedings of the 2017 10th International Conference on Ubi-media Computing and Workshops (Ubi-Media)*, pp. 1–6, IEEE, Pattaya, Thailand, August 2017.

[39] A. S. A. Ali and X. Bao, "Design and research of infrared remote control based on ESP8266," *OALib*, vol. 08, no. 4, pp. 1–14, 2021.

[40] C. Yang, "Design of smart home control system based on wireless voice sensor," *Journal of Sensors*, vol. 2021, Article ID 8254478, pp. 2021–11, 2021.

[41] O. Taiwo and A. E. Ezugwu, "Internet of things-based intelligent smart home control system," *Security and Communication Networks*, vol. 2021, Article ID 9928254, 17 pages, 2021.

[42] C. Stolojescu-Crisan, C. Crisan, and B. P. Butunoi, "An IoT-based smart home automation system," *Sensors*, vol. 21, no. 11, p. 3784, 2021.

[43] R. Singh, P. Kuchhal, A. Gehlot, and S. Choudhury, "Design and implementation of energy efficient home automation system," *Indian Journal of Science and Technology*, vol. 9, no. 6, pp. 1–10, 2016.

[44] M. A. Khan, I. Ahmad, A. N. Nordin et al., "Smart android based home automation system using internet of things (IoT)," *Sustainability*, vol. 14, no. 17, Article ID 10717, 2022.

[45] R. Majeed, N. A. Abdullah, I. Ashraf, Y. B. Zikria, M. F. Mushtaq, and M. Umer, "An Intelligent, Secure, and Smart home Automation System," *Scientific Programming*, vol. 2020, Article ID 4579291, 14 pages, 2020.

[46] W. A. Jabbar, T. K. Kian, R. M. Ramli et al., "Design and fabrication of smart home with internet of things enabled automation system," *IEEE Access*, vol. 7, pp. 144059–144074, 2019.